

1 **Field Investigation of Relationship between Pavement Surface Texture and Friction**

2
3
4 **Sareh Kouchaki**

5 Graduate Research Assistant, S.M. ASCE
6 Department of Civil, Architectural, and Environmental
7 The University of Texas at Austin
8 301e E Dean Keeton St C1700, Austin, TX 78712; E-mail: sareh.kouchaki@utexas.edu
9

10 **Hossein Roshani**

11 Engineer, Ph.D., A.M. ASCE
12 City of San Antonio
13 Streets Engineering & Infrastructure Management
14 Transportation and Capital Improvements (TCI)
15 114 W Commerce St, TX 78205; E-mail: hossein.roshani@sanantonio.gov
16

17 **Jorge A. Prozzi**

18 Professor and Director, International Center for Partnered Pavement Preservation
19 Department of Civil, Architectural, and Environmental
20 The University of Texas at Austin
21 301e E Dean Keeton St C1700, Austin, TX 78712; E-mail: prozzi@mail.utexas.edu
22

23 **Natalia Zuniga-Garcia**

24 Graduate Research Assistant
25 Department of Civil, Architectural, and Environmental
26 The University of Texas at Austin
27 301e E Dean Keeton St C1700, Austin, TX 78712; E-mail: nzuniga@utexas.edu
28

29 **Joaquin Bernardo Hernandez**

30 Research Engineer
31 Center for Transportation Research
32 The University of Texas at San Antonio
33 1616 Guadalupe St, # 4.240, Austin, TX 78701; E-mail: joaquinh@utexas.edu
34

35 **The following paper is a pre-print, the final publication can be found in Transportation**
36 **Research Record, No. 2672: 395–407, 2018.**

37
38 Kouchaki, S., Roshani, H., Prozzi, J. A., Zuniga-Garcia, N., & Hernandez, J. B. (2018). Field
39 Investigation of Relationship between Pavement Surface Texture and Friction. *Transportation*
40 Research Record, 2672(40), 395–407. <https://doi.org/10.1177/0361198118777384>
41

42 **ABSTRACT**

43 Proper tire-pavement interaction is essential for the safety of motorists. Pavement surface texture
44 is a major contributing factor to tire-pavement friction. This study performed a series of statistical
45 analyses of field-measured friction and texture data to find the texture-friction correlation. Three
46 test sections with different pavement types were selected within the state of Texas. Data were
47 collected at three locations in the right wheel path and three locations in the center of the lane for

1 each test section. To measure the texture data, the researchers used the Circular Track Meter (CTM)
2 and a prototype measurement device developed in-house and consisting of a line laser scanner
3 (LLS). Friction measurements were obtained with the Dynamic Friction Tester (DFT) and Grip-
4 Tester. The mean profile depth (MPD) was calculated by using the measured texture data. The
5 relationship between the MPD values and the friction numbers obtained from the Grip-Tester and
6 DFT was investigated at speeds of 50 and 70 km/h (31.1 and 43.5 mph). The repeatability and
7 reliability of both the developed LLS prototype and the Grip-Tester were also evaluated, as well
8 as the effect of test speed on friction measurement. The results indicated a strong positive
9 correlation between the texture and friction data. Additionally, the developed LLS prototype was
10 able to scan the pavement surface texture more reliably and precisely than the CTM in terms of
11 vertical and horizontal resolution. The Grip-Tester showed promising results compared to the DFT
12 with regards to the friction measurement.

13
14 Keywords: Pavement surface texture, friction, Mean profile depth, Grip-Tester, Line laser scanner
15

16 INTRODUCTION

17
18 The direct force developed in the tire-pavement interface is known as *skid resistance*, a property
19 defined by the properties of the tire, the vehicle speed, and the pavement condition and texture.
20 Pavement texture is determinant of the resistance of the pavement surface to a vehicle sliding and
21 skidding (1, 2). The extent of skid resistance on any given pavement is dependent on the design of
22 the surface texture—specifically its micro- and macro-texture—as the texture can affect the skid
23 resistance, splash-and-spray, rolling resistance, and tire wear (3). Pavement design can adjust
24 surface pavement properties to provide the safety needed (4).

25 Pavement surface texture is influenced by many factors, such as aggregate type and size,
26 mixture gradation, and texture orientation, among others. Pavement texture is the result of the
27 deviations of the surface layer from an actual planar surface (5). The World Road Association has
28 categorized pavement texture by a range of wavelength (λ) and amplitudes (A). The standard
29 specification organizations, such as the American Society for Testing Materials (5), International
30 Organization for Standardization (6), and German Institute for Standardization (DIN on ISO
31 13473-1), accepted and incorporated these definitions. The ISO 13473-1 refined the terms
32 incorporating typical amplitudes (7) as follows:

- 33 • Micro-texture ($\lambda < 0.5$ mm, $A = 1$ to 500 μm) (where λ is wavelength and A is amplitude)
- 34 • Macro-texture (0.5 mm $< \lambda < 50$ mm, $A = 0.1$ to 20 mm)
- 35 • Mega-texture (50 mm $< \lambda < 500$ mm, $A = 0.1$ to 50 mm)

36 *Micro-texture* refers to the small-scale texture of the aggregate surface, which controls the
37 contact between the tire rubber and the pavement surface. Micro-texture is a function of aggregate
38 particle mineralogy, petrology, and source (natural or manufactured), and is affected by the
39 environmental effects and the action of traffic (8). *Macro-texture* refers to the large-scale texture
40 of the pavement surface due to the aggregate particle size and arrangement. In asphalt pavements,
41 the mixture properties (aggregate shape, size, and gradation), which define the type of mixture,
42 control the macro-texture (9). Mega-texture has wavelengths in the same order of size as the
43 tire/pavement interface. Examples of mega-texture include ruts, potholes, and major joints and
44 cracks. It affects vibration in the tire walls but not the vehicle suspension, and it is therefore
45 strongly associated with noise and rolling resistance (9).

1 Pavement friction is the result of a complex interplay between two principal frictional force
2 components: adhesion and hysteresis. Although there are other components of pavement friction,
3 such as tire rubber shear, they are insignificant when compared to the adhesion and hysteresis force
4 components (3, 9). Thus, friction can be viewed as the sum of adhesion and hysteresis. *Adhesion*
5 is the friction that results from the small-scale bonding/interlocking of the vehicle tire rubber and
6 the pavement surface. It is a function of the interface shear strength and contact area (9, 10). The
7 *hysteresis* component of the frictional forces results from the energy loss created within the tire as
8 it responds to the texture. Because the adhesion force is developed at the tire/pavement interface, it
9 is most responsive to the micro-level asperities (micro-texture) of the aggregate particles. In
10 contrast, the hysteresis force developed within the tire is most responsive to the macro-level
11 asperities (macro-texture) formed in the pavement surface. Thus, in principle, adhesion governs
12 the overall friction on smooth-textured and dry pavements, while hysteresis is the dominant
13 component on wet and rough-textured pavements (3, 9).

14 In 2015, Torbruegge and Wies in Germany studied the correlation between wet skid
15 resistance and pavement texture. Their findings showed no correlation between the mean texture
16 depth (MTD) as a surface texture characteristic and skid resistance as measured by British
17 pendulum (11). Similar results were obtained by Gunaratne et al. in which no significant
18 correlation was found between friction and MTD. However, Gunaratne et al. observed a strong
19 correlation between friction and the texture frequency characteristics, such as the power spectral
20 density calculated by fast Fourier transform (12).

21 The precise nature of the relationship between friction and texture remains unknown,
22 although several attempts to reveal it have been made using methods such as Fourier, wavelet, and
23 fractal analysis (13-15). These models' degree of complexity and the difficulty in finding the
24 coefficients relating to the calculations results in complications for road engineers.

25 **GOAL AND OBJECTIVES**

26 Understanding the texture-friction relationship is valuable for transportation agencies and
27 engineers for proper pavement maintenance and better design of pavement, especially when higher
28 skid resistance is needed. A few studies have been conducted in this regard, but the effects of
29 pavement texture on the friction produced at the pavement surface are still not fully understood.
30 This study's primary goal is to find the correlation between field-measured texture and friction
31 data. For this purpose, several objectives were defined:

- 32 • Develop an accurate texture measurement device, called a line laser scanner (LLS) prototype,
33 and evaluate its performance by comparing its results to those of the CTM.
- 34 • Use the Grip-Tester to collect continuous friction data at traffic speed and compare it to the
35 DFT at two different speeds.
- 36 • Calculate the MPD values of texture data and perform statistical analysis to establish
37 correlations between texture and friction.

38 **EXPERIMENTAL METHODS AND THEORETICAL EVALUATIONS**

39 **Measurement of Skid Resistance**

40 There are three main skid resistance measuring principles: longitudinal friction coefficient (LFC),
41 transverse, and stationary or slow-moving (16, 17). The LFC measurement principle aims to
42 measure friction when a vehicle is traveling forward in a straight line. When the brakes are applied,
43 both the angular velocity of the wheel and the overall velocity of the vehicle decrease. When the
44 braking force on the wheels is too strong, the wheels are "locked" and consequently slide over a

1 surface. LFC measurement devices have slip ratios that simulate the wheel slipping process when
2 a wheel slides over a surface. More specifically, the slip ratio compares the vehicle's velocity to
3 the angular velocity of the wheel. When the slip ratio is 0, the angular velocity of the wheel is the
4 same as the velocity of the vehicle (i.e., no slip between wheel and surface). When the slip ratio is
5 1, there is no angular velocity in the wheel (i.e., wheel is fully locked and slides over the surface).
6 LFC devices can have either a fixed or a variable slip ratio (15, 17).

7 The stationary or slow-moving measurement principle is used in compact devices usually
8 found in the laboratory or still testing. One such device uses a pendulum arm; others, such as the
9 DFT, use a rotating head. Both devices use rubber sliders that use the surface friction to slow down
10 the pendulum or the rotating head (16-18).

11 Table 1 summarizes LFC measurement devices commonly used around the world. LFC
12 devices can measure between 5 and 140 km/h (5.1 and 87 mph) and can come in the form of
13 compact trailers or large-capacity trucks. LFC devices use a watering system, requiring vehicles
14 to carry a water tank for measurement purposes. Transverse friction measurement devices are
15 usually larger, more expensive, and can take measurements for longer distances since greater water
16 capacity increases maximum measurement distance. While inexpensive and easy to use, stationary
17 or slow-moving devices must be operated manually (18).

18

1

Table 1 Comparison of the LFC Measuring Devices (16-18)

Device Name	Theoretical water film thickness (WFT), Speed, Tire type, Measurement interval (Interval)	Assembly	Device Picture
ADHERA	TWFT: 1 mm Speed: 40–120 km/h Tire type: Smooth PIARC tire 165R15 Interval: 20 m Country/Countries of Use: France	Assembly: Trailer that can be hooked up to vehicle Commercially Available: No	
BV-11	TWFT: 1 mm Speed: 20–160 km/h [C] Tire type: Trelleborg tire T49 Interval: 20 m Country/Countries of Use: England, Sweden, and Finland	Assembly: Trailer that can be hooked up to vehicle Commercially available: Yes	
Grip-Tester	TWFT: 0.5 mm Speed: 5–100 km/h Tire type: Smooth ASTM tire, 254 mm diameter Interval: 10 or 20 m Country/Countries of Use: United States, United Kingdom, and others	Assembly: Trailer that can be hooked up to vehicle. Commercially available: Yes	
ROAR DK	WFT: 0.5 mm Speed: 60–80 km/h Tire type: ASTM 1551 Interval: 5m + Country/Countries of Use: Denmark	Assembly: Trailer that can be hooked up to a vehicle Commercially available: No	
ROAR NL	TWFT: 0.5 mm Speed: 50–70 km/h Tire type: ASTM 1551 Interval: 5–100 m Country/Countries of Use: Netherlands	Assembly: Three-axle tanker truck with two measuring systems mounted at the rear of the chassis. (Tank capacity is about 12,000 liters.) Commercially available: No	
RWS NL	TWFT: 0.5 mm Speed: 50 – 70 km/h Tire type: PIARC smooth 165 R15 Interval: 5 – 100 m Country/Countries of Use: Netherlands	Assembly: Trailer that can be hooked up to a vehicle. Commercially Available: No	

Skiddometer BV-8	TWFT: 0.5 mm Speed: 40–80 km/h TT: AIPCR ribbed, 165 R15, with four longitudinal grooves Interval: 30–50 m Country/Countries of Use: Sweden	Assembly: Trailer that can be hooked up to a vehicle Commercially available: Yes	
SRM	TWFT: 0.5 mm Speed: 40–80 km/h TT: AIPCR ribbed, 165 R15, with four longitudinal grooves Interval: 20 m Country/Countries of Use: Germany	Assembly: The test wheels are mounted on the back of a tanker vehicle at the approximate location of a vehicle tire paths. Commercially available: No	
TRT	WFT: 0.5 mm Speed: 40–140 km/h Tire type: Smooth ASTM Interval: Typically, 20 m Country/Countries of Use: Czech Republic	Assembly: The measuring equipment is under a specially equipped vehicle Commercially available: No	
SRT-3	WFT: 0.5 mm Speed: 30–90 km/h Tire type: Tire with thread (200kPa) Interval: 100 m Country/Countries of Use: Poland	Assembly: Trailer that can be hooked up to a vehicle Note: SRT-3 is more sensitive to micro-texture changes than to macro- texture changes. Commercially Available: No	
IMAG	WFT: 1.0 mm Speed: up to 140 km/h Tire type: PIARC smooth profile tire Interval: N/A Country/Countries of Use: France, Germany, and Poland	Assembly: Trailer that can be hooked up to a vehicle Commercially available: Yes	
ICC	WFT: 1.0 mm Speed: 65 to 80 km/h Country/Countries of Use: United States, and others	Assembly: Trailer that can be hooked up to vehicle Commercially available: Yes	

1
2 Among the measurement devices presented in Table 1, the Grip-Tester was selected
3 because it showed the most promise for measuring pavement friction because of its wider range of
4 test speed, better repeatability and reproducibility (depending on the operating speed), greater
5 efficiency in water usage, and commercial availability (18). The Grip-Tester is a friction-
6 measuring trailer that uses a fixed slip wheel to simulate anti-lock braking on a wet road surface.
7 This is achieved by the Grip-Tester having three wheels: two have patterned treads and are

1 connected by a drive axle, while the third is a smooth tread tire. The drive axle, connecting the two
2 drive wheels, has a 27-tooth sprocket; it is connected by a transmission chain to the measuring
3 wheel that has a 32-tooth sprocket (19). The difference in sprocket teeth creates a 15% continuous
4 slippage on the measurement tire. To create wet road conditions, a watering system supplies a
5 constant water thickness specified by the user to the measuring wheel.

6 The axle connecting the measuring wheel outputs the dynamic friction by using strain
7 gages to measure the horizontal drag force and vertical load force. The information is used to
8 estimate the Grip Number (GN), or coefficient of friction, in real-time. (19). As shown in Equation
9 1, the GN is the ratio between the fraction of tractive drag force (F_d) and the load force (Q).

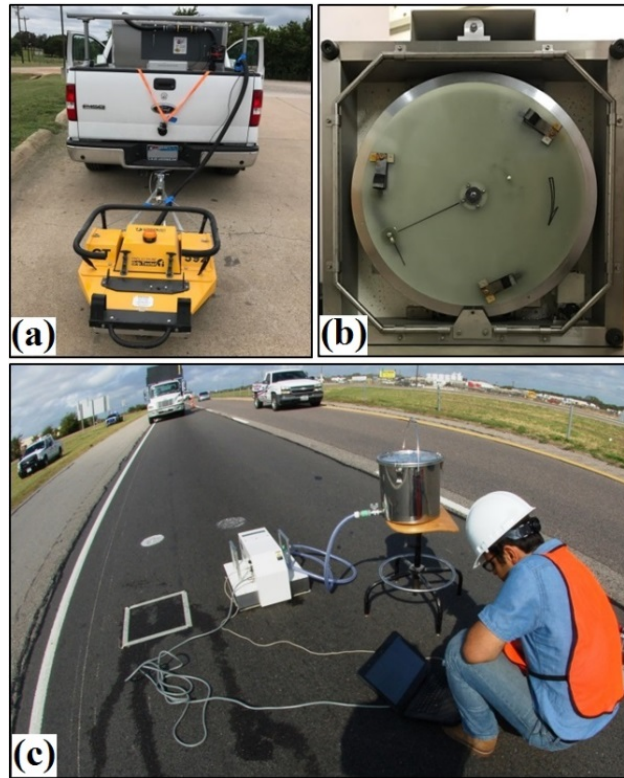
$$11 \quad GN = \frac{F_d}{Q} \quad (1)$$

12
13 The Grip-Tester (Figure 1(a)) needs a vehicle capable of towing the trailer as well as a
14 water tank to supply water to the measuring wheel.

15 Along with the Grip-Tester, the DFT was used to measure the friction of the pavement at
16 different speeds. This machine is specified under ASTM E1911. The DFT (shown in Figures 1(b)
17 and 1(c)) consists of a rotating disk and three rubber pads attached to the bottom of the disk. The
18 disk is pushed by an electric motor to rotate until it reaches the target speed set by an operator. At
19 the same time, water is applied to the pavement surface. The disk drops and the rubber pads come
20 into contact with the wet area. Each rubber pad is loaded vertically at 11.8 N (2.65 lb). The friction
21 force developed between pads and the pavement slows down the disk. The DFT measures the
22 friction coefficient continuously until the disk stops completely (13, 20). The coefficient of friction
23 (μ) is the ratio between the friction force or horizontal torque force (F) and the applied vertical
24 load on the rubber sliders of the DFT (21).

$$25 \quad \mu = \frac{F}{Q} \quad (2)$$

27

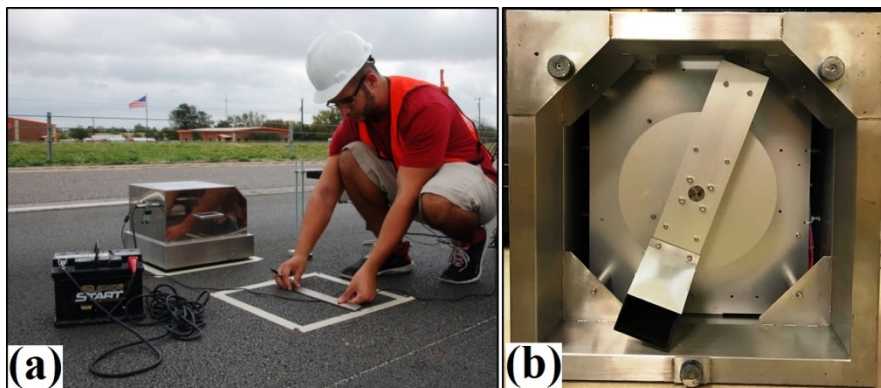


1
2 **Figure 1 a) The Grip-Tester attached to a vehicle, b) bottom view of the DFT, and c) the**
3 **DFT connected to a water tank and DCC measuring the friction at the lane center path.**
4

5 **Measurement of Pavement Surface Texture**

6 ***Circular Track Meter (CTM)***

7 CTM is a common static method used to measure the macro-texture of the pavement surface.
8 According to the ASTM E2157, the CTM (Figures 2(a) and 2(b)) consists of a laser-displacement
9 sensor that rotates over a circle with a diameter of 284.5 mm (11.2 in.) and measures the profile of
10 pavement surface texture. The profile includes 1024 points scanned at an interval of 0.87 mm
11 (0.034 in.). Using the instructions provided by ASTM E 1845, the measured profile then is
12 sectioned into eight equal parts and the highest profile peak in each part is measured (23, 24).
13



14 **Figure 2 a) The CTM powered by a battery measuring the texture at the right wheel path,**
15 **and b) bottom view of the CTM.**
16

1
2
3
4
5
6
7
8
9
10
11

Developed Line Laser Scanner (LLS) Prototype

LLS was utilized in this research study to scan the pavement texture. This device is two-dimensional non-contact laser sensor that projects blue light in a horizontal line. Small changes in the height due to the texture irregularities can also be captured using this scanner system (25). A prototype (Figure 3(a)) was developed to enable LLS to capture three-dimensional data. For this purpose, the LLS was mounted on a linear motion controller (linear stage) to travel over the surface and scan it at a given interval. Figure 3(c) illustrates the picture of the triangulation system. Due to the angle between the camera and the laser, the system could miss data from vertical edges.

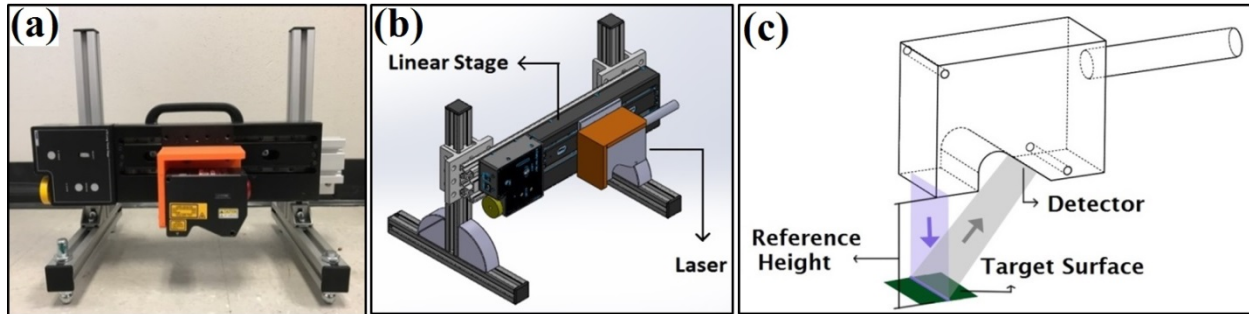


Figure 3 a) A front view of the LLS prototype, b) a 3-D schematic view of the LLS, and c) the triangulation system of laser.

12
13
14
15

Calculation of Mean Profile Depth (MPD)

In 1992 the Permanent International Association of Road Congresses (PIARC) performed an experiment using 41 friction and texture measuring devices in Spain and Belgium. The results of that experiment showed the MPD parameter as the best pavement macro-texture indicator (23). The MPD is estimated from the surface height profile following ASTM E1845. The first step is to censor the inclination slope of the height profile such that a regression line is calculated and then subtracted from the height profile and so the initial profile will be converted to a zero-mean profile. As a second step (Figure 4), the height profile is divided into two segments with the length of $\frac{L}{2}$ for which the maximum height is detected. By using Equation 3, MPD is calculated as the average of the two determined maximum heights.

26
27
28

$$MPD = \frac{Max\ Height\ of\ 1st\ Segment + Max\ Height\ of\ 2nd\ Segment}{2} \quad (3)$$

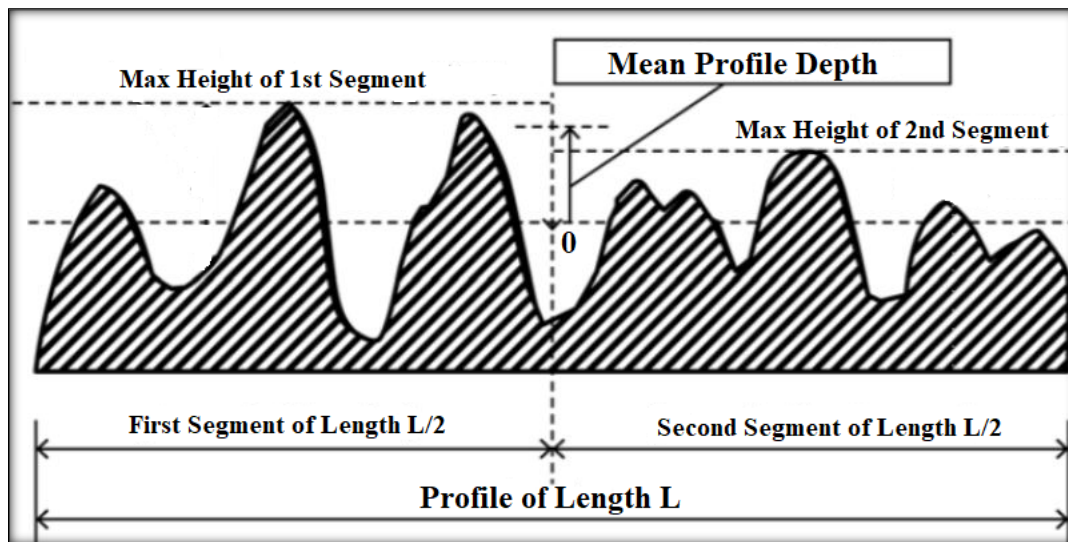


Figure 4 Graphical illustration of MPD calculation (26).

1
2
3
4
5
6
7
8
9
10
11
12
13
14
15
16
17
18
19
20
21
22
23
24

Field-Data Collection

Test sections and pavement type

Three test sections, each more than five years old, were selected. Each section had established measurement data for the DFT, CTM, and LLS. The sections chosen provide a variety of mix designs, ensuring variation of surface texture for the test. The test sections are located in Bastrop, Bryan, and Fort Worth:

- Bastrop:
 - o Mix design: Porous Friction Course (PFC)
 - o Average annual daily traffic (AADT): 13,972
- Bryan:
 - o Mix design: Dense-Graded Type C
 - o AADT: 5,843
- Fort Worth:
 - o Mix design: Dense-Graded Type D
 - o AADT: 57,385

At each location, six samples were taken: three in the right wheel path and three in the center of the lane, with a 12.5 m (41 ft) distance between the locations (Figure 5). Within each location, one CTM and one DFT measurements were obtained. The CTM and DFT testing followed ASTM E2157 and ASTM E1911 procedures, which state the equipment should be placed in the same location.

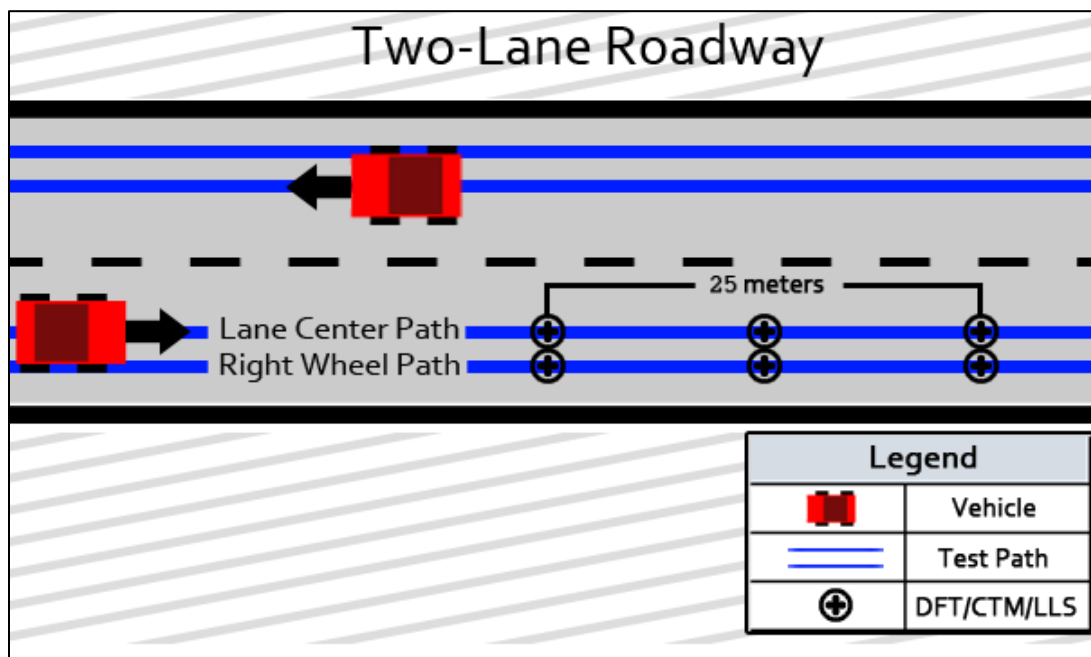


Figure 5 Illustration of test section and test location.

To maintain consistency in the surface measurements, the LLS was placed in the same locations described for the CTM. Note, however, that these devices operate differently due to the mechanism of motion in each: the CTM measures in a circle and the LLS measures linearly. For the CTM, eight segments of 111.5 mm (4.39 in.) arcs are scanned by the laser, which results in a full circle. To ensure an equitable comparison with the CTM's measurements, the LLS was configured to scan a 120 mm (4.72 in.) length at a linear speed of 8 mm/s (0.31 in./s) with a sampling frequency of 1 kHz. The area scanned by the LLS was the same as the segment of the CTM that was parallel to the direction of traffic.

For the Grip-Tester, the test consisted of two target speeds (50 km/h and 70 km/h) to evaluate the dependency of speed on friction. The speed needs to be maintained within 5% of the target speed. The 70 km/h (43.5 mph) target was selected to enable a direct comparison to the DFT equipment, which has a speed range of up to 80 km/h (49.7 mph).

RESULTS AND DISCUSSIONS

Repeatability of Developed LLS Prototype

The LLS results were compared to those from the CTM to investigate the repeatability and reliability of the developed LLS. The MPD, as a surface characteristic, was calculated for all test locations. Then, single values of MPD for the right wheel path and the center were obtained by averaging the three respective samples. This was done for both LLS and CTM as graphed in Figure 6(a)—the -R and -C represent the right wheel path and lane center path, respectively. As this figure illustrates, the MPD values obtained by the LLS, denoted as *MPD-by-LLS*, are very close to the MPD values of CTM, denoted as *MPD-by-CTM*. There were no observable biases between the MPD values with which to draw a general conclusion.

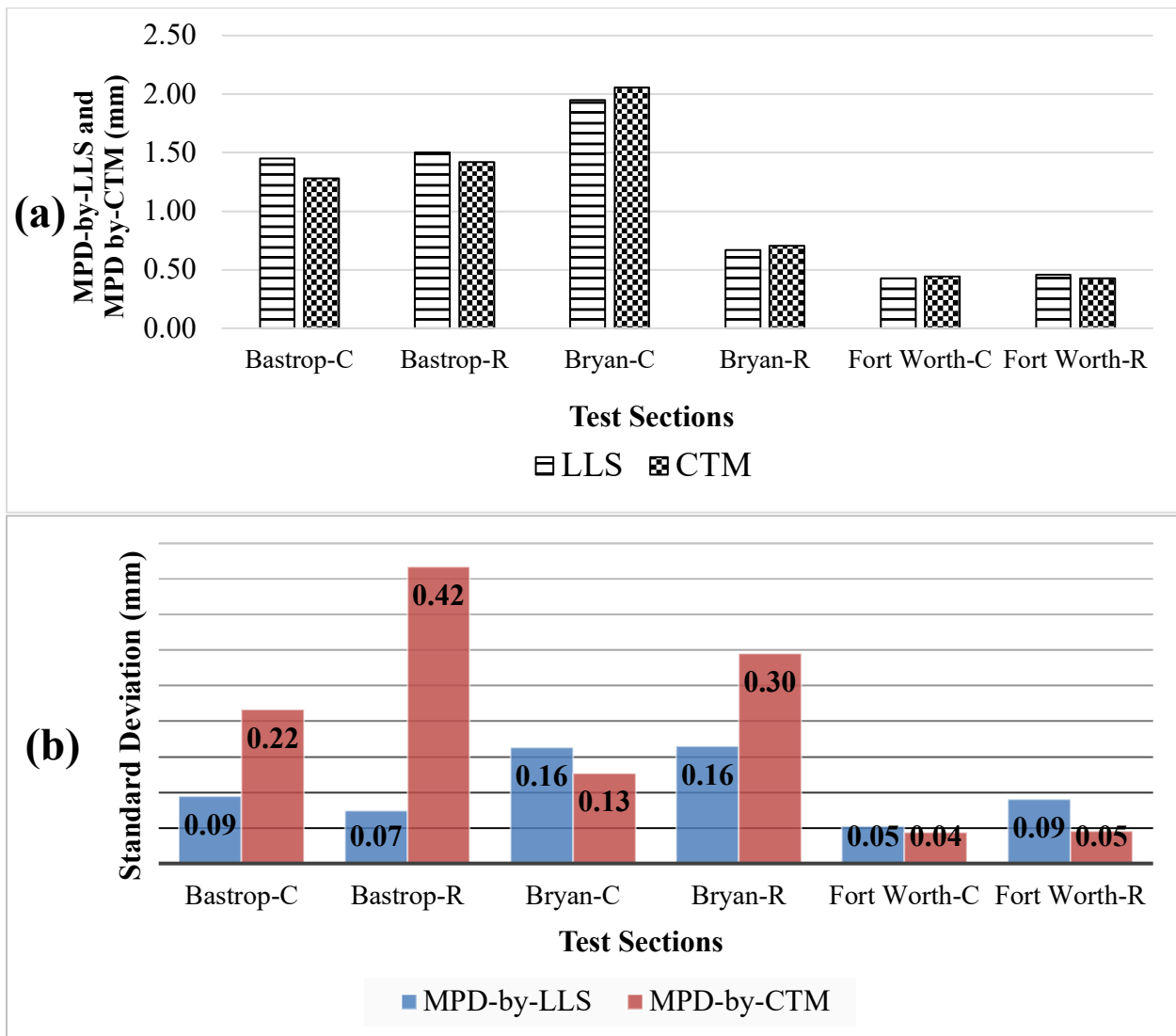


Figure 6 a) Comparison of mean MPD values obtained from developed LLS prototype and CTM, b) Standard deviation of MPD values measured by developed LLS prototype and CTM at six test sections.

Repeatability of the developed LLS prototype was evaluated by calculating the average and standard deviation of three MPD-by-LLS and MPD-by-CTM values obtained at each test section from their respective test paths. Then, the standard deviation of each group of data was compared. For example, the three MPD-by-LLS values for the pavement surface under the right wheel path at the Bryan test section were compared to each other with respect to their standard deviation. Due to the short distance between test locations, similar texture characteristics were expected at those locations. As Figure 6(b) indicates, the standard deviations of MPD-by-LLS data were significantly lower than MPD-by-CTM in three test sections (Bastrop-R, Bastrop-C, and Bryan-R). Comparable MPD values were observed at the rest of the sections. According to these results, one can suggest that the developed LLS prototype is capable of providing an accurate and precise measurement of the pavement surface texture.

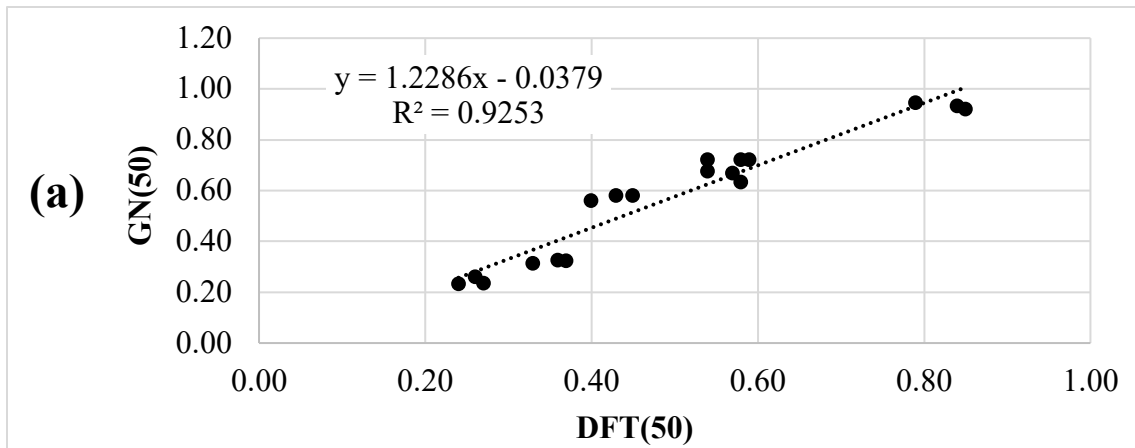
1 **Grip-Tester Results**

2 Figures 7(a) and 7(b) show the GN of all test locations plotted against the DFT values at two
3 different speeds of 50 and 70 km/h (31.1 and 43.5 mph). As these figures illustrate, the GN values
4 have a strong relationship with DFT values, with R^2 of 0.93 and 0.91 at the two different speeds.
5 It can be concluded that this relationship is independent of the test speed.

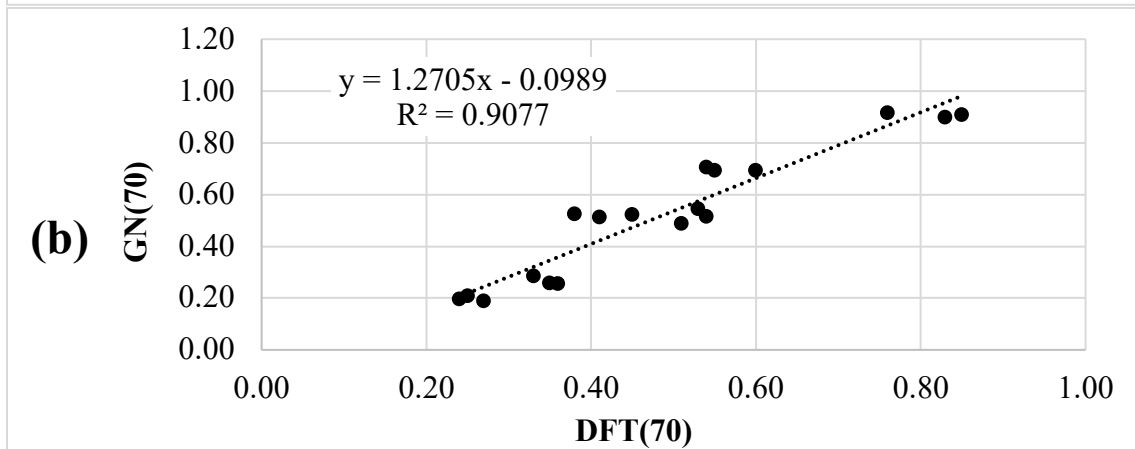
6 These findings indicate that the Grip-Tester is a reliable alternative for the DFT and does
7 not require traffic control, therefore, it is safer and more efficient. Besides, the Grip-Tester enables
8 engineers to obtain continuous friction data over a long pavement section.

9 Based on the literature, no given speed has been specified by agencies to perform the test.
10 Hence, understanding the effect of speed on GN, would help researchers and practitioners interpret
11 the friction results in different cases when the test speed is a variable. The results plotted in Figure
12 7(c) show that the GN decreased when the speed increased. This finding is reasonable but contrasts
13 with the results of a study conducted at the University of Auckland by Wilson et al. in 2013, in
14 which they stated that at speeds less than 75 km/h, the GN may not be affected by test speeds (27).
15

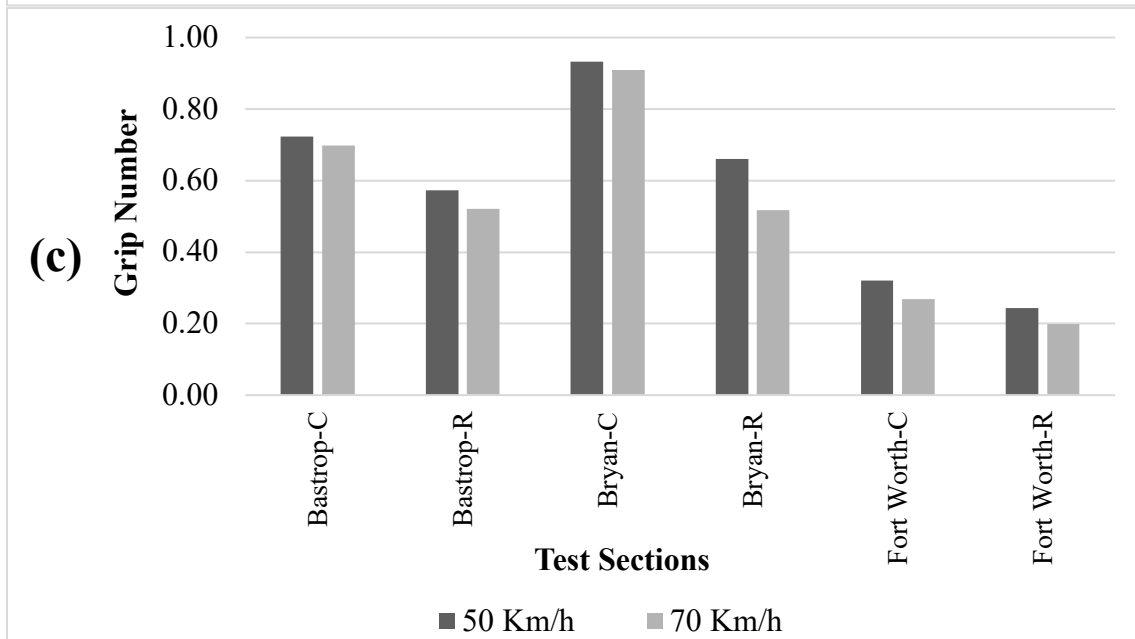
1



2



3



4

5 **Figure 7 Correlation between GN and DFT values at two speeds of a) 50 km/h and b) 70**
 6 **km/h, and c) the Grip number at different test sections.**

7

8

According to Figure 6(a), the MPD value of the section Bryan-R, which is about 0.70 mm

1 (0.027 in.), is lower than Bastrop-R with MPD of 1.50 mm (0.06 in.). However, interestingly, in
2 Figure 7(c), the GN at Bryan-R is higher than that of Bastrop-R. It should be mentioned that, in
3 these test locations, the water film thickness of 0.5 mm (applied by Grip-Tester) can only cover a
4 portion of surface texture depth. The PFC pavement is an open-graded friction course that allows
5 drainage of water through the asphalt layer. The surface pavement type of the Bastrop test section
6 is PFC; therefore, the lack of small-size aggregates results in higher MPD values. On the other
7 hand, the mix design of the Bryan test section is dense-graded type C, which contains all ranges
8 of aggregate size and thus results in a lower MPD value but a greater tire-pavement contact area.
9 In this case, it can be suggested that the adhesion factor is decisive in friction.

10 Although a PFC mix design increases the surface MPD (and thus causes more hysteresis),
11 PFC's design also decreases the chance of the aggregates being fully exposed and coming into
12 contact with the tire (thus decreasing the contact area and adhesion). A smooth surface is associated
13 with more contact area and better adhesion, but it significantly decreases the MPD that results in
14 lower hysteresis. Therefore, the balance between adhesion and hysteresis in the pavement surface
15 should be optimized in order to maximize the surface friction and skid resistance. This is
16 achievable by using an appropriate mix design providing both macro-texture and micro-texture
17 (15).

18 The lowest friction was observed in the Fort Worth test sections where the MPD values
19 were below 0.46 mm (0.018 in.). Considering the water film thickness of 0.5 mm (0.019 in.)
20 applied by the Grip-Tester for wetting purpose, it can be concluded that the surface texture was
21 fully covered by water. In this case, the water trapped in the V- or U-shaped areas of the pavement
22 surface bears the load from the tire and prevents the tire penetrating the spaces between the
23 aggregates—thus reducing the contribution of the aggregate surface to the friction force by
24 decreasing the tire-aggregate contact area (28).

26 Relationship between the Texture and Friction

27 The GN and DFT values both represent the friction properties of the pavement surface; however,
28 the MPD values obtained by the LLS and CTM reflect the texture characteristics of the surface.
29 To explore the relationship between the friction and texture, those two groups were plotted against
30 each other in four different forms: GN vs. CTM, GN vs. LLS, DFT vs. CTM, and DFT vs. LLS.

31 Using statistical analysis, the correlation coefficient (R) was used to evaluate the
32 relationships. The R ranges from -1 to +1, where negative and positive signs represent the negative
33 or positive linear correlation respectively.

34 The statistical analysis shows that the relationship between the GN values and MPDs is
35 strongly linear with high correlation coefficients (Figure 8). For the Grip-Tester performed at 50
36 km/h, the $R = 0.83$ was found for GN-CTM, and $R = 0.82$ for GN-LLS. In addition, higher
37 correlation coefficients were observed at the speed of 70 km/h. The R values of 0.88 and 0.89 show
38 a strong linear relationship between GN as a friction parameter, and MPDs of CTM and LLS,
39 respectively.

40 From the results provided in Figure 8, the Grip-Tester data have a better relationship with
41 texture compared to the DFT data in terms of the calculated R^2 values. Thus, it can be suggested
42 that friction and skid resistance could be estimated by means of texture measurement data with
43 high confidence.

44

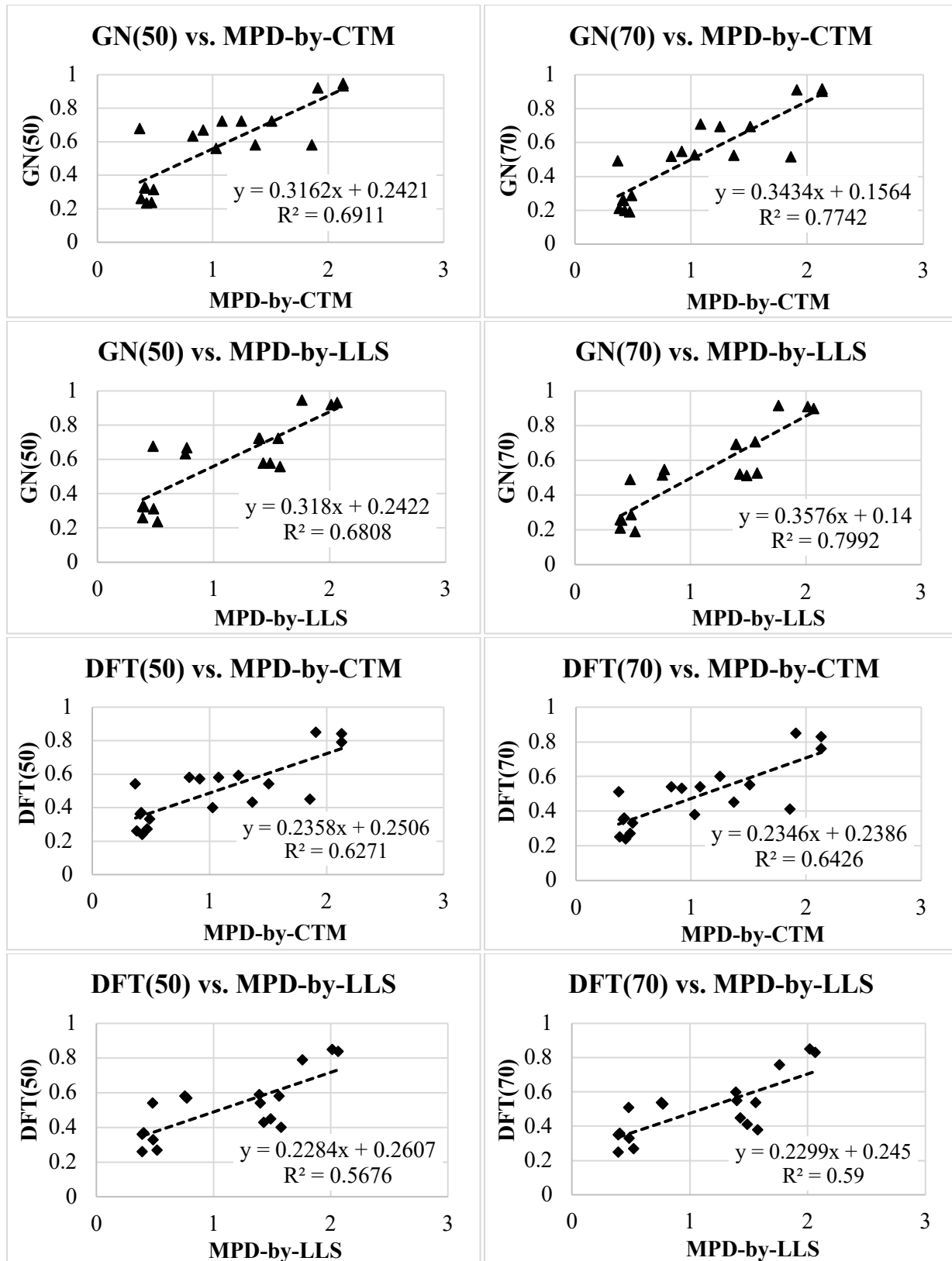


Figure 8 Plotted texture-friction data points including GN, DFT values, and MPD values.

1
2
3
4
5
6

1 CONCLUSIONS

2 This study investigated the relationship between the texture and friction of pavement surfaces
3 using field-measured data. During this study, a texture scanner prototype—the LLS—was
4 developed to measure the texture data along with the CTM. The MPD was adopted as a pavement
5 texture indicator. DFT and Grip-Tester were employed for friction measurement. The efficiency
6 and repeatability of the developed LLS were explored through comparison to the CTM results.

7 The results of the repeatability analysis and standard deviation showed the reliability of the
8 developed LLS prototype for texture measurement. In all the test sections, the MPD calculated
9 from the LLS data was similar to that calculated from the CTM data. Therefore, it is recommended
10 that the developed LLS prototype should be considered as an efficient alternative to the CTM
11 device, especially when three-dimensional texture data are needed.

12 Regardless of the test speed and pavement type, the friction number obtained by the Grip-
13 Tester showed a strong linear correlation with DFT measurements. Due to the reliable results of
14 the Grip-Tester, its wider range of friction measurement, and the lack of need to control traffic,
15 this device is recommended for use by state DOTs for friction measurement. The quality of the
16 friction data obtained by a Grip-Tester seems to be somewhat sensitive to the test speed, because
17 the GN decreased slightly when the test speed increased from 50 km/h to 70 km/h (31.1 mph to
18 43.5 mph). This finding implies that keeping the test speed fixed at different test sections is
19 important to achieving comparable results.

20 This study's statistical analysis findings pointed to a strong positive linear correlation
21 between texture and friction in pavements. The highest linear correlation coefficients (R) were
22 observed between the GNs obtained at 70km/h (43.5 mph) and texture data obtained using either
23 the LLS or the CTM. The authors of this study recommend running the Grip-Tester at higher speeds
24 in cases when the texture-friction relationship analysis is the point of interest. As a further
25 recommendation, accurate friction prediction models could be developed based on the texture
26 measurement data to eliminate the need for direct friction measurement.

28 REFERENCES

- 29 1. Asi, I.M. Evaluating skid resistance of different asphalt concrete mixes. *Journal of Building*
30 *and Environment*. Vol. 42, 2007, pp. 325–329.
- 31 2. Wang, H., and Z. Wang. Evaluation of pavement surface friction subject to various pavement
32 preservation treatments. *Journal of Construction and Building Materials*. Vol. 48, 2013, pp. 194–
33 202.
- 34 3. Henry, J.J. *NCHRP Synthesis of Highway Practice 291: Evaluation of Pavement Friction*
35 *Characteristics*. Transportation Research Board, National Research Council, 2000.
- 36 4. Hoerner, T.E., and K. D. Smith. *High performance concrete pavement: Pavement texturing and*
37 *tire-pavement noise*. Publication FHWA-DTFH61-01-P-00290. FHWA, U.S. Department of
38 Transportation, 2002.
- 39 5. *Standard Terminology Relating to Vehicle-Pavement Systems*. ASTM E867 – 2012, Philadelphia,
40 Pennsylvania, American Society for Testing and Materials.
- 41 6. *Characterization of Pavement Texture by Use of Surface Profiles*. ISO 13473-1, 1997,
42 International Organization for Standardization.
- 43 7. Sandberg, U. Influence of Road Surface Texture on Traffic Characteristics Related to
44 Environment, Economy, and Safety: A State-of-Art-Study Regarding Measures and measuring
45 Methods. *VTI notat53A-1997*, 1998, Swedish National Road Association, Linkoping, Sweden.

- 1 8. Kogbara, B.R., E.A. Masad, E. Kassem, A.T. Scarpas, and K. Anupam. A state-of-the-art review
2 of parameters influencing measurement and modeling of skid resistance of asphalt pavements.
3 *Journal of Construction and Building Materials*, Vol. 114, 2016, pp. 602–617.
- 4 9. Hall, J.W., K.L. Smith, L. Titus-Glover, L.D. Evans, J.C. Wambold, and T.J. Yager. *NCHRP*
5 *Project 01-43: Guide for Pavement Friction*. Transportation Research Board, Washington, D. C.,
6 2009.
- 7 10. Gunaratne, M., N. Bandara, J. Medzorian, M. Chawla, and P. Ulrich. Correlation of Tire Wear
8 and Friction to Texture of Concrete Pavements. *Journal of Materials in Civil Engineering*, Vol. 12,
9 2000, pp. 46-54.
- 10 11. Stefan Torbruegge, S., and B. Wies. Characterization of pavement texture by means of height
11 difference correlation and relation to wet skid resistance. *Journal of Traffic and Transportation*
12 *Engineering*, Vol. 2, 2015, pp. 59-67.
- 13 12. Gunaratne, M., N. Bandara, J. Medzorian, M. Chawla, and P. Ulrich. Correlation of tire wear
14 and friction to texture of concrete pavements. *Journal of Materials in Civil Engineering*, Vol. 12,
15 No. 1, 2000.
- 16 13. Huang, H. and J. Pan. Speech pitch determination based on Hilbert–Huang transform. *Journal*
17 *of Signal Processing*, Vol. 86, 2006, pp. 792–803.
- 18 14. Rado, Z. and M. Kane. An initial attempt to develop an empirical relation between texture and
19 pavement friction using the HHT approach. *Wear*, Vol. 309, 2014, pp. 233–246.
- 20 15. Kane, M., I. Artamendi, and T. Scarpas. Long-term skid resistance of asphalt surfacings:
21 correlation between Wehner– Schulze friction values and the mineralogical composition of the
22 aggregates. *Wear*, Vol. 303, 2013, pp. 235–243.
- 23 16. Descornet, G., B. Schmidt, M. Boulet, M. Gothie, M.T. Do, J. Fafie, M. Alonso, P. Roe, R.
24 Forest, and H. Viner. HERMES Project: Harmonization of European Routine and research
25 Measuring Equipment for Skid Resistance. FEHRL report, 2006.
- 26 17. Do, M.T., and P. Roe, Report on state-of-the-art of test methods. TYROSAFE project
27 deliverable D04, 2008.
- 28 18. Andriejauskas, T., V. Vorobjovas, and V. Mielonas. Evaluation of skid resistance characteristics
29 and measurement methods”, 9th International Conference of Environmental Engineering, Vilnius,
30 Lithuania, 2014.
- 31 19. Thomas, L. Grip-Tester MK2 D-type Maintenance Manual. Issue 4, Findlay, Irvine Limited,
32 Scotland, 2008.
- 33 20. Masad, E., A. Rezaei, A. Chowdhury, and P. Harris. *Predicting Asphalt Mixture Skid*
34 *Resistance Based on Aggregate Characteristics*. FHWA/TX-09/0 5627-1. FHWA, Texas A&M
35 University, 2009.
- 36 21. *Guide to the Management of Road Surface Skid Resistance*. Sydney, Australia: Austroads,
37 2005.
- 38 22. Wambold, J.C., C.E. Antle, J.J. Henry, and Z. Rado. International PIARC experiment to
39 compare and Harmonize texture and skid resistance measurements. PIARC Technical Committee
40 on Surface Characteristics, Madrid, 1995.
- 41 23. Abbas, A., M.E. Kutay, H. Azari, and R. Rasmussen. Three-Dimensional Surface Texture
42 Characterization of Portland Cement Concrete Pavements. *Journal of Computer-Aided Civil and*
43 *Infrastructure Engineering*, Vol. 22, 2007, pp: 197–209.
- 44 24. Mataei, B., H. Zakeri, M. Zahedi, and F. M. Nejad. Pavement Friction and Skid Resistance
45 Measurement Methods: A literature Review. *Journal of Civil Engineering*, Vol. 6, 2016, pp.537-
46 565.
- 47 25. KEYENCE, *Measurement Sensors*, <http://www.keyence.com/products/measure/index.jsp>,

- 1 Accessed on January 1, 2017.
- 2 26. *Standard Practice for Calculating Pavement Macrotexture Mean Profile Depth*. ASTM E1845
- 3 – 2015, Philadelphia, Pennsylvania, American Society for Testing and Materials.
- 4 27. Wilson, D.J., B. Jacobsen, and B. Chan. *NZ Transport Agency research report 523: The effect*
- 5 *of road roughness (and test speed) on GripTester measurements*. NZ Transport Agency, 2013.
- 6 28. Meegoda, J.N., and G. Shengyan. Evaluation of pavement skid resistance using high speed
- 7 texture measurement. *Journal of Traffic and Transportation Engineering*, Vol. 2 (6), 2015, pp. 382-
- 8 390.